

## THE MAGNETIC HYPERFINE FIELD AT $^{140}\text{Ce}$ IN NICKEL

A.G. BIBILONI \*, M.C. CARACOCHE \*\*, A.R. LOPEZ GARCÍA \*,  
J.A. MARTINEZ \*\*, L.A. MENDOZA ZELIS \*\*, R.C. MERCADER \*  
and A.F. PASQUEVICH \*\*\*

*Departamento de Física, Facultad de Ciencias Exactas, Universidad Nacional de La Plata,  
La Plata, Argentina*

Received 8 May 1978

The hyperfine interaction of  $^{140}\text{Ce}$  in nickel has been investigated by the time-differential perturbed-angular-correlation technique (TDPAC). The probe was produced by isotope separator implantation of the fission product  $^{140}\text{Xe}$ , the  $\beta^-$  decay chain of which finally populates excited states of  $^{140}\text{Ce}$ .

Different spin rotation spectra were observed before and after an 8 h annealing at  $415^\circ\text{C}$ . The analysis of the spectra led to the conclusion that the Ce ions were in the diamagnetic  $4^+$  state. The dominant contributions to the hyperfine interaction are two different magnetic hyperfine fields:  $|H_{\text{hf}}^1| = 385 \pm 7$  kOe and  $|H_{\text{hf}}^2| = 276 \pm 12$  kOe.  $H_{\text{hf}}^1$  disappears after annealing. The fraction of nuclei which observe  $H_{\text{hf}}^2$  is increased by the annealing procedure from 16% to 75%. It is assumed that  $H_{\text{hf}}^1$  is the hyperfine field of CeNi in an unperturbed substitutional site and  $H_{\text{hf}}^2$  is attributed to Ce ions which have trapped a single vacancy.

### 1. Introduction

When impurity atoms are introduced in a given lattice by implantation, the nature of the sites reached can be determined in certain cases with the aid of the nuclear time-differential perturbed-angular correlation (TDPAC) technique [1–3].

The ratio of the atomic sizes of impurity and host is connected to the probability of finding a substitutional undisturbed site for the implanted atom [2]. Provided the implantation temperature allows vacancy migration, the mismatch of large impurities in ferromagnetic hosts makes it possible that the implanted ions trap vacancies formed close to them during implantation. Several sites can therefore be reached according to the number of defects trapped and their distances to the

\* Member of Carrera del Investigador Científico, CONICET, Argentina.

\*\* Member of Carrera del Investigador Científico de la Comisión de Investigaciones Científicas de la Provincia de Buenos Aires, Argentina.

\*\*\* Fellow of Comisión de Investigaciones Científicas de la Provincia de Buenos Aires, Argentina.

impurity. When the impurity and the defect concentrations are sufficiently small, the trapping of a radiation damage defect by the impurity will produce very definite changes in the hyperfine interaction parameters.

In our investigation, in which the  $^{140}\text{Ce}$  activity is obtained via  $\beta^-$  decay of  $^{140}\text{Xe}$  impurities implanted in a polycrystalline nickel lattice, the ratio of atomic sizes between implanted impurities and host favours the vacancy trapping mechanism.

It is not well established experimentally whether Ce impurities in metals behave as rare earth trivalent ions, which show a localized magnetic moment due to their 4f electron, or as diamagnetic  $4^+$  ions [4–11]. In the following we briefly describe the possible behaviours of Ce ions in ferromagnetic hosts.

(a) The hyperfine interaction experienced by rare earth impurities implanted in ferromagnetic cubic hosts has been extensively studied [11,12]. The interpretation of the results becomes complicated owing to the fact that besides the radiation damage associated to the implantation, crystalline electric field and relaxation effects are present.

When relaxation effects can be neglected and first order perturbation theory is used, the exchange interaction between the localized 4f moment and the polarized conduction electrons at the host and the crystalline field interaction leads to a combined static magnetic and electric quadrupole hyperfine interaction. In principle, all spectra of rare earth trivalent ions in nickel show the presence of at least two components, each one characterized by a hyperfine magnetic field and a quadrupole interaction. One of them corresponds to impurities in damaged non-substitutional sites with a strong axial crystal field in which the electronic ground state has  $|\langle J_z \rangle| \approx J$  and  $|\langle J_z^2 \rangle| \approx J^2$ , so that the hyperfine parameters  $H_{\text{hf}}$  and  $V_{\text{zz}}$  have the free ion values. The other stems from impurities in substitutional sites and, due to the fact that in nickel the exchange field may be comparable in magnitude with the crystal field, the corresponding hyperfine parameters are reduced relative to the former ones.

The correct assignment of the substitutional or non-substitutional character to these interactions can be tested by annealing treatments. It is well known that the population of the substitutional sites gradually decreases when the source is annealed within a certain temperature range [3,11–15].

When available, channeling results and/or resistivity data may help explain both components dependence on annealing temperature through vacancy migration and trapping mechanisms.

Niesen et al. [11,12], using the Mössbauer effect technique, have determined the hyperfine parameters and population fractions of two different sites for various rare earth ions implanted in nickel host. In all cases the above description is confirmed.

(b) Let us now analyze what we must expect if cerium impurities implanted in nickel host behave as diamagnetic ions.

TDPAC and Mössbauer effect hyperfine studies of large non-magnetic impurities implanted in ferromagnetic hosts show the existence of various components corre-

sponding to different hyperfine fields [16–22]. Calculations based on three- and four-component models where the highest magnetic frequency is ascribed to nuclei in non-perturbed substitutional sites and the others to nuclei at sites of lower symmetry, i.e. with one, two or more neighbouring vacancies, have thrown light on experimental results. That is the case of Mössbauer measurements of  $^{131}\text{I}$  and  $^{125}\text{I}$  impurities [19] and  $^{133}\text{Xe}$  impurities [20] implanted in the iron host.

Under favourable conditions, the electric quadrupole frequencies due to loss of cubic symmetry at each perturbed site, may be observed.

Relaxation effects are excluded due to the absence of 4f electrons.

Kugel et al. [23] have determined the induced hyperfine magnetic fields at  $^{142}\text{Ce}$  in Fe, Co and Ni hosts at room temperature by means of the time integral IMPAC technique. The analysis of Ce in Fe results suggests that the orbital angular momentum of the 4f shell is unable to dominate the observed hyperfine field. From their measurement, a hyperfine magnetic field of  $-94.5$  kOe in nickel may be deduced though this value is affected by a large uncertainty.

Spanjaard et al. [24], using the NO technique, have reported preliminary experimental results on the hyperfine magnetic field acting on  $^{137\text{m}}\text{Ce}$  impurities implanted in Fe and Ni foils. The data in Ni are approximately fitted with a field of  $135 \pm 20$  kOe. In these experiments nothing is reported about possible quadrupole contributions. The signs of the determined hyperfine fields are opposite to what one expects from an antiferromagnetic coupling between the iron and the rare earth spins suggesting that cerium behaves in these cases as a diamagnetic  $4^+$  ion.

The aim of this work is to study the hyperfine interaction of  $^{140}\text{Ce}$  ions implanted in a nickel host with the purpose of clarifying the magnetic behaviour of cerium impurities in this lattice.

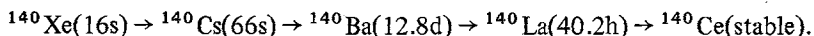
In sect. 2 the experimental procedure and data handling are described and in sect. 3 the results obtained are reported. Finally, sect. 4 presents an analysis of these results in terms of the predictions described here, which leads to the conclusions in sect. 5.

## 2. Experimental procedure

The source was prepared by implanting  $^{140}\text{Xe}$  into a thin polycrystalline, high-purity (99.99%) nickel backing by the IALE project isotope separator [25] at an energy of 60 keV.

The oxide layers were removed mechanically from the nickel foil and then the  $^{140}\text{Xe}$  activity was implanted during about two days due to the low beam intensity available.

$^{140}\text{Xe}$  was produced by  $^{235}\text{U}$  fission and the  $^{140}\text{Ce}$  activity to be studied is obtained via the  $\beta^-$  cascade:



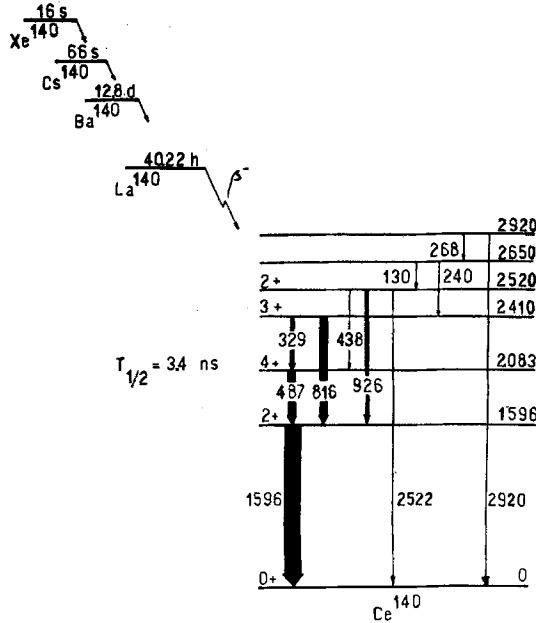


Fig. 1. Partial level scheme of  $^{140}\text{Ce}$  populated in the decay of  $^{140}\text{La}$ .

The long-lived parent  $^{140}\text{Ba}$  allows precise measurements in spite of the low activity which we obtained.

For our TDPAC experiment, the 328.6–486.7 keV  $\gamma\text{-}\gamma$  cascade in the decay product  $^{140}\text{Ce}$  was used. Fig. 1 shows the low energy level scheme of  $^{140}\text{Ce}$ . The selected cascade has an intermediate level of energy 2083 keV, half-life 3.45 ns, nuclear gyromagnetic factor  $g = 1.11 \pm 0.04$  [4] and electric quadrupole moment  $Q = 0.404 \pm 0.080$  b [26].

Implantation as well as subsequent TDPAC experiments were carried out at room temperature. Two series of measurements were performed during approximately 15 days each, namely: (A) immediately after implantation and (B) after annealing the source during 8 hours at  $415^\circ\text{C}$ .

The conventional angular correlation apparatus consisted of two  $5 \times 5$  cm NaI(Tl) detectors and fast-slow electronics as usual. Time resolution was 2.2 ns.

The coincidence spectra  $C(\theta, t)$  obtained show the typical decay due to the lifetime  $\tau$  of the intermediate level modulated by the perturbed angular correlation function  $W(\theta, t)$ :

$$C(\theta, t) = A e^{-t/\tau} W(\theta, t),$$

For a polycrystalline source we have the well-known time-dependent angular correlation function:

$$W(\theta, t) = \sum_k A_{kk} G_k(t) P_k(\cos \theta),$$

where  $P_k(\cos \theta)$  are the Legendre polynomials and  $A_{kk}$  the angular correlation coefficients experimentally determined to be [4]:

$$A_{22} = -0.105 \pm 0.003, \quad A_{44} = -0.001 \pm 0.002.$$

$G_k(t)$  are related to the perturbations arising from the hyperfine interaction in the intermediate level of the cascade and in this way, they give information about the extranuclear fields acting on the TDPAC probe nuclei.

If the time spectra are taken at only two fixed angular positions on account of the low value of  $A_{44}$ , i.e.  $\theta = \frac{1}{2}\pi$  and  $\theta = \pi$ , the ratio

$$R(t) = 2 \frac{C(\pi, t) - C(\frac{1}{2}\pi, t)}{C(\pi, t) + C(\frac{1}{2}\pi, t)}$$

eliminates the exponential decay factor and may be well approximated by the expression:

$$R(t) \approx \frac{3}{2} A_{22} G_2(t).$$

Finally, a least-squares fitting of this function allows the determination of the perturbation factor  $G_2(t)$ .

Previous Fourier analysis of the experimental data is usually carried out in order to estimate the frequencies of the various Fourier components which one may expect from the least-squares fitting of the  $R(t)$  function.

### 3. Results

Experimental  $R(t)$  values are shown in fig. 2 for both series of measurements: (A) before annealing and (b) after annealing at  $415^\circ\text{C}$ .

The experimental results were analyzed taking into account the two possible configurations of the  $^{140}\text{Ce}$  ion, i.e.  $\text{Ce}^{3+}$  and  $\text{Ce}^{4+}$ .

A first attempt to fit the experimental points with a curve fulfilling the rare earth requirements described in sect. 1(a) was made, which assumed: (a) two inequivalent sites for the cerium impurities, (b) a combined static magnetic and electric quadrupole interaction at each site, (c) the possible distribution of the interaction frequencies and (d) a relaxation factor which took into account the possibility of an electronic correlation time  $\tau_c$  not negligible with respect to the nuclear Larmor period  $\tau_n$ . The corresponding perturbation factor is

$$G_2(t) = \sum_{i=1}^2 f^{(i)} [s_{20} + 2 \cos(\omega_B^{(i)} t) \sum_n s_{2n} \cos(n\omega_0^{(i)} t) + 2 \cos(2\omega_B^{(i)} t) \sum_{n'} s_{2n'} \cos(n'\omega_0^{(i)} t)] e^{-\lambda_c^{(i)} t},$$

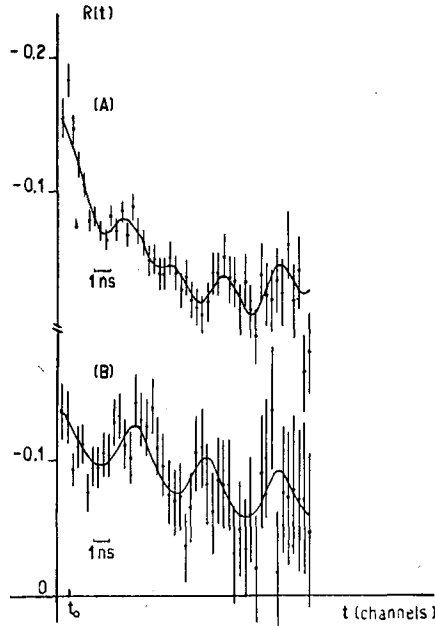


Fig. 2. TDPAC spectra of  $^{140}\text{Ce}$  implanted in Ni. (A): before annealing, (B): after 8 h annealing at  $415^\circ\text{C}$ .

where  $\omega_0 = \frac{3}{112} eQV_{zz}/\hbar$  and  $\omega_B = g\mu_N H/\hbar$  represent the quadrupole and the Larmor precession frequencies respectively.  $s_{2n}$  and  $s_{2n'}$  are the coefficients of the axially symmetric quadrupole interaction in a polycrystalline source calculated according to ref. [27]. The summation index  $n$  runs over odd values while  $n'$  runs over even ones.  $f^{(1)}$  and  $f^{(2)} = 1 - f^{(1)}$  are the fractions of nuclei in substitutional and non-substitutional positions, respectively.

The requirement (c) was fulfilled assuming a frequency distribution of Lorentzian shape and the relaxation mechanism was taken into account through a multiplying factor of the form  $e^{-\lambda_c t}$  where  $\lambda_c$  is connected to the correlation time  $\tau_c$ .

No satisfactory fits were obtained. Moreover, the hypothesis that the lowest frequency is the substitutional one does not agree with this frequency behaviour shown with annealing.

A second attempt, in which a theoretical curve was fitted which assumes diamagnetic behaviour for the cerium impurities described in sect. 1(b), was quite successful, however. Several different sites were considered for the  $\text{Ce}^{4+}$  ions. The corresponding perturbation factor is:

$$G_2(t) = \sum_i f^{(i)} [1 + 2 \cos(\omega_B^{(i)} t) + 2 \cos(2\omega_B^{(i)} t)],$$

where  $\omega_B^{(i)}$  and  $f^{(i)}$  characterize the Larmor frequency and population fraction

Table 1  
Hyperfine fields and site populations obtained for  $^{140}\text{Ce}$  impurities in nickel

Measurement	$H_{\text{hf}}^{(\text{h})}$ (kOe)	$f^{(\text{h})}$	$H_{\text{hf}}^{(\text{i})}$ (kOe)	$f^{(\text{i})}$	$H_{\text{hf}}^{(1)}$ (kOe)	$f^{(1)}$
(A)	$385 \pm 7$	$0.58 \pm 0.06$	$276 \pm 12$	$0.16 \pm 0.05$	$37 \pm 2$	$0.26 \pm 0.04$
(B)			$273 \pm 7$	$0.75 \pm 0.07$	$27 \pm 5$	$0.25 \pm 0.06$

respectively of each inequivalent site. A Lorentzian frequency distribution is again assumed in this fit.

The solid curves of fig. 2 are the best fits got. They involve three magnetic frequencies, the so-called high, intermediate and low components [19]. The widths of all three interaction frequencies are zero.

Reasonable agreement was obtained between the Fourier analysis and the least-squares results.

In table 1 are listed the magnetic hyperfine fields  $H_{\text{hf}}$  and the population fractions  $f$  corresponding to each site for both sets of experiments (A) and (B).

#### 4. Discussion

According to the discussion in 1(b) for large diamagnetic impurities implanted in ferromagnetic hosts, the highest hyperfine field corresponds to substitutional sites and weaker fields to perturbed sites associated to one or more neighbouring vacancies.

In the frame of this hypothesis our results can be interpreted in the following way: After the implantation (see analysis of curve (A)) 58% of the probe ions occupy unperturbed substitutional sites with the high magnetic hyperfine field and 16% have trapped a single vacancy and observe the intermediate field. The remaining ions may have trapped several vacancies or occupy a site at a grain boundary. The annealing treatment reinforces the vacancy trapping mechanism. In the situation of the measurement (B), all ions have left the unperturbed substitutional site and 75% of the ions have now trapped a single vacancy. The population of the weak field site has not changed.

The observed dependence of the substitutional component on the annealing temperature is in accordance with Bernas' group investigations which show that in Ni vacancy associated migration takes place in the annealing stage around  $500^\circ\text{C}$  [3,14,15].

Our conclusion that after annealing 75% of the Ce ions have trapped a single vacancy implies, of course, that these nuclei see also a strong electric field gradient.

In the point charge approximation, this field gradient is given by

$$V_{zz}^{1v} = \frac{Q_{\text{eff}}^{1v}}{4\pi\epsilon_0 r^3} 2P_2(\cos\theta)(1 - \gamma_\infty)(1 - K).$$

Inserting  $Q_{\text{eff}}^{1v} = 2e$ ,  $\gamma_\infty = -66.79$  [28] and  $1 - K \simeq 2$  [29], one obtains for a nearest neighbour vacancy:

$$V_{zz}^{1v} = 5.04 \times 10^{18} \text{ V/cm}^2.$$

This value agrees fairly well with the one deduced from the experimental electric field gradient for a nearest neighbour vacancy trapped by In impurities in a Pt lattice [30]. In fact, taking into account the different lattice parameters, Sternheimer factors and intermediate levels quadrupole moments and spins, the quadrupole interaction frequency for the  $4^+$  state of  $^{140}\text{Ce}$  in the nickel host becomes:

$$\omega_0 = 30.1 \text{ Mhz.}$$

This frequency is so small that one can be sure that the electric interaction is not responsible for the periodic structure of the spin rotation pattern observed.

## 5. Conclusions

From the results reported in the previous sections we conclude that we observe from the TDPAC spectra the Ce ions in the  $4^+$  ionization state. This is the ionization state which is primarily produced by the  $\beta^-$  decay of the 40 h mother isotope  $^{140}\text{La}$ , provided the equilibrium ionization state of La in Ni is  $3^+$ .

Our result means therefore that the nickel host is not a fast reducing agent for cerium impurities in contrary to other host metals [6,7].

If our interpretation of the spectra is correct, the magnetic hyperfine field of Ce in Ni at unperturbed substitutional sites must be:

$$|H_{\text{hf}}| = 385 \pm 7 \text{ kOe.}$$

We are greatly indebted to Prof. Erwin Bodenshtedt for helpful discussions and comments on this work.

We also thank Dr. D. Otero, Ing. R. Requejo and Mr. J. Cava from the Comisión Nacional de Energía Atómica de la República Argentina, for the isotope separator implantations and Ing. G. Cusminsky from the Departamento de Metalurgia de la Facultad de Ingeniería de la Universidad Nacional de La Plata for helping us with the annealing treatment.

Partial financial support of the Organization of American States, CONICET and Comisión de Investigaciones Científicas de la Provincia de Buenos Aires are gratefully acknowledged.



## References

- [1] H. de Waard, *Phys. Scripta* 11 (1975) 157.
- [2] G. Vogl, *Hyperfine Interactions* 2 (1976) 151.
- [3] H. Bernas, *Rev. de Phys. Appl.* 9 (1974) 575.
- [4] H.J. Körner, E. Gerdau, C. Günther, K. Auerbach, G. Mielken, G. Strube and E. Bodenstedt, *Z. Phys.* 173 (1963) 203.
- [5] M. Schmorak, H. Wilson, P. Gatti and L. Grodzins, *Phys. Rev.* B134 (1964) 718.
- [6] S.G. Cohen, N. Kaplan and S. Ofer, in *Perturbed angular correlations*, eds. E. Karlsson, E. Mathias and K. Siegbahn (North-Holland, Amsterdam, 1964) p. 313.
- [7] R.M. Levy and D.A. Shirley, *Phys. Rev.* B140 (1965) 811.
- [8] E. Bodenstedt, in *Perturbed angular correlations*, eds. E. Karlsson, E. Mathias and K. Siegbahn (North-Holland, Amsterdam, 1964) p. 217.
- [9] B. Coqblin and A. Blandin, *Adv. in Physics* 17 (1968) 281.
- [10] S. Koicki and A. Koicki, *Z. Phys.* 255 (1972) 216.
- [11] L. Niesen, *Hyperfine Interactions* 2 (1976) 15.
- [12] L. Niesen, P.J. Kikkert and H. de Waard, *Hyperfine Interactions* 3 (1977) 109.
- [13] L. Niesen and H.P. Wit, *J. de Phys., Colloque C6, supplément au Tome 37*, p. C6-639, 1976.
- [14] F. Abel, M. Bruneaux, C. Cohen, J. Chaumont, L. Thomé and H. Bernas, *Solid State Commun.* 13 (1973) 113.
- [15] H. Bernas, *Phys. Scripta* 11 (1975) 167.
- [16] M. Rots and R. Coussement, *J. de Phys.* 35 (1974) C1-35.
- [17] R. Coussement, G. Dumond, G. Langouche, H. Pattyn, M. Rots, K.P. Schmidt and M. Van Rossum, *J. de Phys.* 35 (1974) C1-37.
- [18] E.N. Kaufmann, J.M. Poate and W.M. Augustyniak, *Phys. Rev.* B7 (1973) 951.
- [19] H. de Waard, R.L. Cohen, S.R. Reintsema and S.A. Drentje, *Phys. Rev.* B10 (1974) 3760.
- [20] S.R. Reintsema, S.A. Drentje, P. Schurer and H. de Waard, *Rad. Effects* 24 (1975) 145.
- [21] C. Hohenemser, A. Arends and H. de Waard, *Phys. Rev.* B11 (1975) 4522.
- [22] *Proc. Conf. on Hyperfine Interactions, Leuven, 1975*, *Hyperfine Interactions* 2 (1976) pp. 198, 355, 356, 358, 362, 365 and 367.
- [23] H.W. Kugel, T. Polga, R. Kalish and R.R. Borchers, in *Hyperfine Interactions in excited nuclei*, ed. G. Goldring and R. Kalish (Gordon and Breach, New York, 1971) p. 104.
- [24] D. Spanjaard, R.A. Fox, J.D. Marsh and N.J. Stone, see ref. [23], p. 113.
- [25] E. Achtemberg, F.C. Iglesias, A.E. Jech, A. Kasulin, E. Kerner, G. Monico, J.A. Moragues, D. Otero, M.L. Perez, M. Pina Monti, A.N. Proto, R. Requejo, J.J. Rossi, W. Scheuer and G.F. Suarez, *Nucl. Instr.* 101 (1972) 555.
- [26] B. Klemme and H. Miemczyk, *J. Phys. Soc. Jap.* 34 (1973) 265.
- [27] H. Frauenfelder and R.M. Steffen, in *Alpha, beta and gamma-ray spectroscopy*, ed. K. Siegbahn, vol. 2 (North-Holland, Amsterdam, 1968).
- [28] F.D. Feiock and W.R. Johnson, *Phys. Rev.* 187 (1969) 39.
- [29] P. Raghavan, E.N. Kaufmann, R.S. Raghavan, E.J. Ansaldo and R.A. Naumann, *Phys. Rev.* B13 (1976) 2835.
- [30] H.G. Müller and K. Krusch, in *4th Int. Conf. on hyperfine interactions, Madison, New Jersey, June 1977*, p. 160 and *Hyperfine Interactions* 4 (1978) 697.